Supplementary Information

The influence of *trans*-ligand to NO to the thermal stability of side-bond coordinated isomer MS2

Artem A. Mikhailov[a], Gennadiy A. Kostin[a], Dominik Schaniel[b]

[a] Nikolaev Institute of Inorganic Chemistry, Siberian Branch of the Russian Academy of Sciences, 3 Acad. Lavrentiev Avenue, Novosibirsk 630090, Russian Federation

[b] Universite´ de Lorraine, CNRS, CRM2, UMR 7036, Nancy 54000, France

Table S1. Experimental and refinement details.

Complex	$[RuNOPy_4F](PF_6)_2 \cdot 0.33H_2O$	$[RuNOPy_4F](PF_6)_2 \cdot 1.5CH_3CN$
Empirical formula	$C_{20}H_{20.67}F_{13}N_5O_{1.33}P_2Ru$	$C_{46}H_{49}F_{26}N_{13}O_2P_4Ru_2$
Formula weight	762.42	1636.00
Temperature/K	150.0	150.0
Crystal system	triclinic	monoclinic
Space group	P-1	$P2_1/c$
a/Å	13.9264(5)	20.7752(13)
b/Å	16.9480(7)	15.3676(9)
c/Å	19.8185(8)	19.9513(9)
α/°	66.7760(10)	90
β/°	79.868(2)	99.0464(15)
γ/°	84.6740(10)	90
Volume/Å^3	4230.2(3)	6290.5(6)
Z	6	4
ρ_{calc}g/cm^3	1.796	1.727
μ/mm^{-1}	0.782	0.708
F(000)	2264.0	3256.0
Crystal size/mm^3	0.114 × 0.083 × 0.082	0.12 × 0.1 × 0.01
Radiation	MoKα (λ = 0.71073)	MoKα (λ = 0.71073)
2Θ range for data collection/°	3.908 to 55.066	3.362 to 48.854
Index ranges	-18 ≤ h ≤ 18, -22 ≤ k ≤ 22, -25 ≤ l ≤ 25	-24 ≤ h ≤ 24, -17 ≤ k ≤ 17, -22 ≤ l ≤ 21
Reflections collected	63937	61086
Independent reflections	19420 [R_{int} = 0.0459, R_{sigma} = 0.0514]	10293 [R_{int} = 0.1148, R_{sigma} = 0.0769]
Data/restraints/ parameters	19420/29/1184	10293/0/841
Goodness-of-fit on F^2	1.200	1.016
Final R indexes [I>=2σ (I)]	R_1 = 0.0813, wR_2 = 0.1596	R_1 = 0.0579, wR_2 = 0.1342
Final R indexes [all data]	R_1 = 0.0992, wR_2 = 0.1661	R_1 = 0.0928, wR_2 = 0.1575
Largest diff. peak/hole / e Å^{-3}	1.57/-1.11	1.05/-0.73

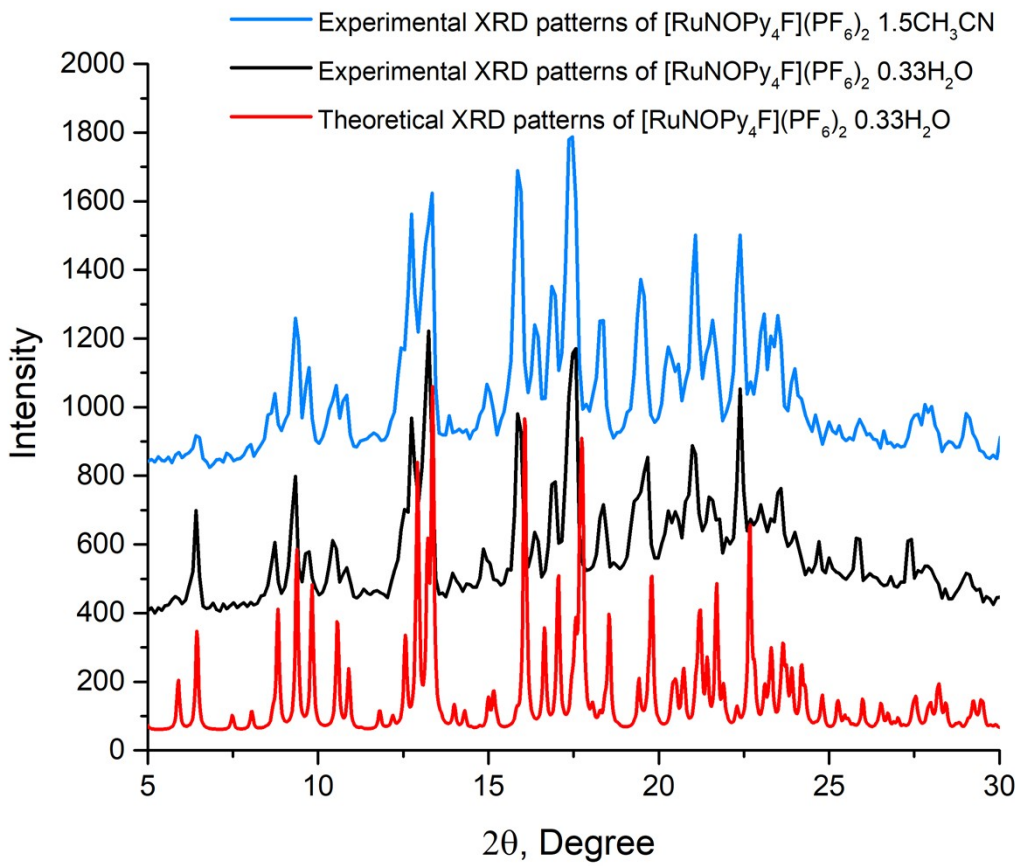

Fig. S1. Comparison of experimental powder XRD patterns of $[RuNOPy_4F](PF_6)_2 \cdot 0.33H_2O$ (**RuF**) and *trans*-$[RuNOPy_4F](PF_6)_2 \cdot 1.5CH_3CN$ with theoretical XRD patterns of $[RuNOPy_4F](PF_6)_2 \cdot 0.33H_2O$ obtained from single crystal XRD.

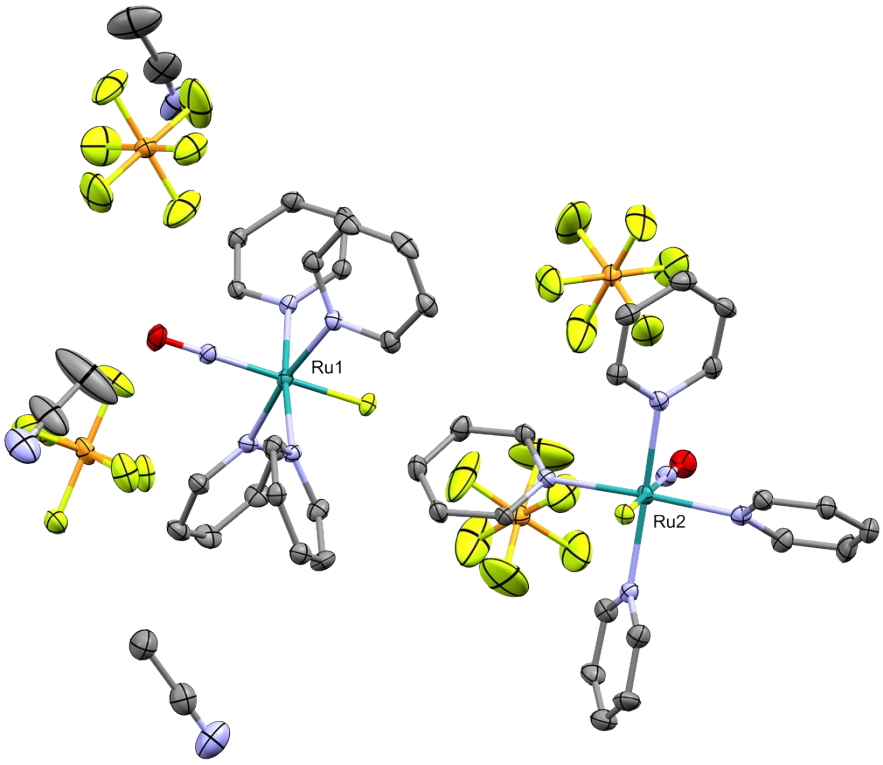

Fig. S2. The structure of *trans*-$[RuNOPy_4F](PF_6)_2 \cdot 1.5CH_3CN$ with two crystallographically independent ruthenium units. Hydrogen atoms are omitted for clarity. Thermal ellipsoids are given at the 30% probability level.

Table S2. Chosen interatomic distances [Å] and angles [°] in *trans*-[RuNOPy$_4$F](PF$_6$)$_2$·1.5CH$_3$CN.

	Ru1 unit	Ru2 unit
Ru-NO	1.749(6)	1.730(6)
N-O	1.128(8)	1.142(9)
Ru-F	1.914(3)	1.915(3)
Ru-N$_{Py}$	2.078(4); 2.091(5); 2.084(6); 2.094(5)	2.094(6); 2.080(6); 2.101(6); 2.100(6)
Ru-N-O	174.0(6)	176.7(6)

Table S3. Chosen bond distances of [RuNOPy$_4$X](PF$_6$)$_2$ (X = F$^-$, Cl$^-$, Br$^-$ and OH$^-$) complexes. Temperatures of the measurements are indicated in the table (T, K).

	N-O	Ru-NO	Ru-X	Ru-Py$_{average}$	T, K	Ref.
RuF*	1.14(1); 1.145(9)	1.731(8); 1.733(6)	1.902(4); 1.910(4)	2.089	150	Present work
RuCl	1.146(2); 1.147(2)	1.755(2); 1.754(2)	2.321(1); 2.323(1)	2.108	180	[1]
RuOH	1.145(4)	1.757(3)	1.910(2)	2.103	293	[2]
RuBr	1.131(4)	1.752(3)	2.466(1)	2.108	180	[1]
* In case of **RuF** complex distances of Ru1 and Ru2 units are considered.						

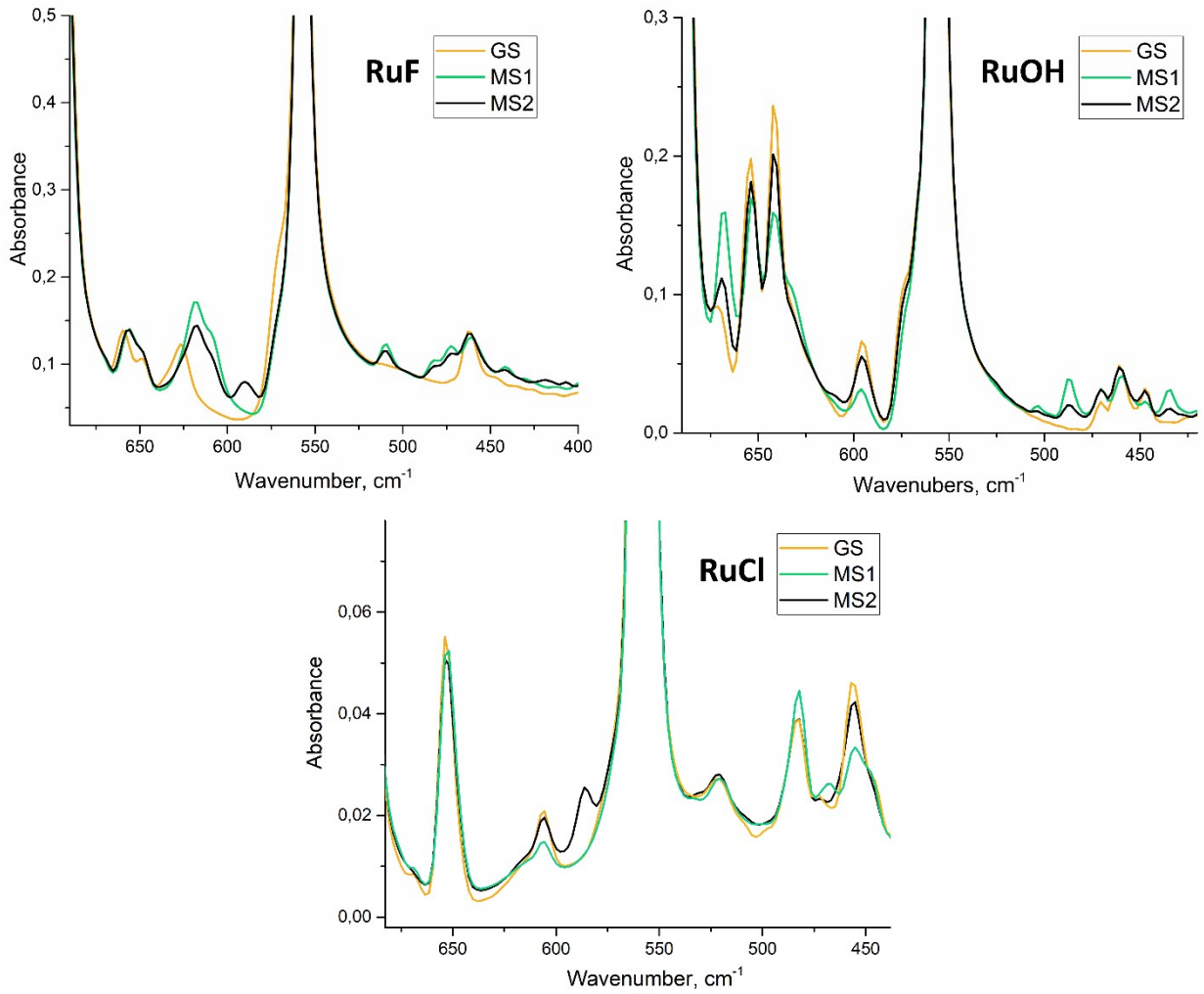

Fig. S3. IR spectra of studied complexes in GS, MS1 and MS2 at 100 K. Strong band at 550 cm^{-1} corresponds to vibration of PF_6^- anion.

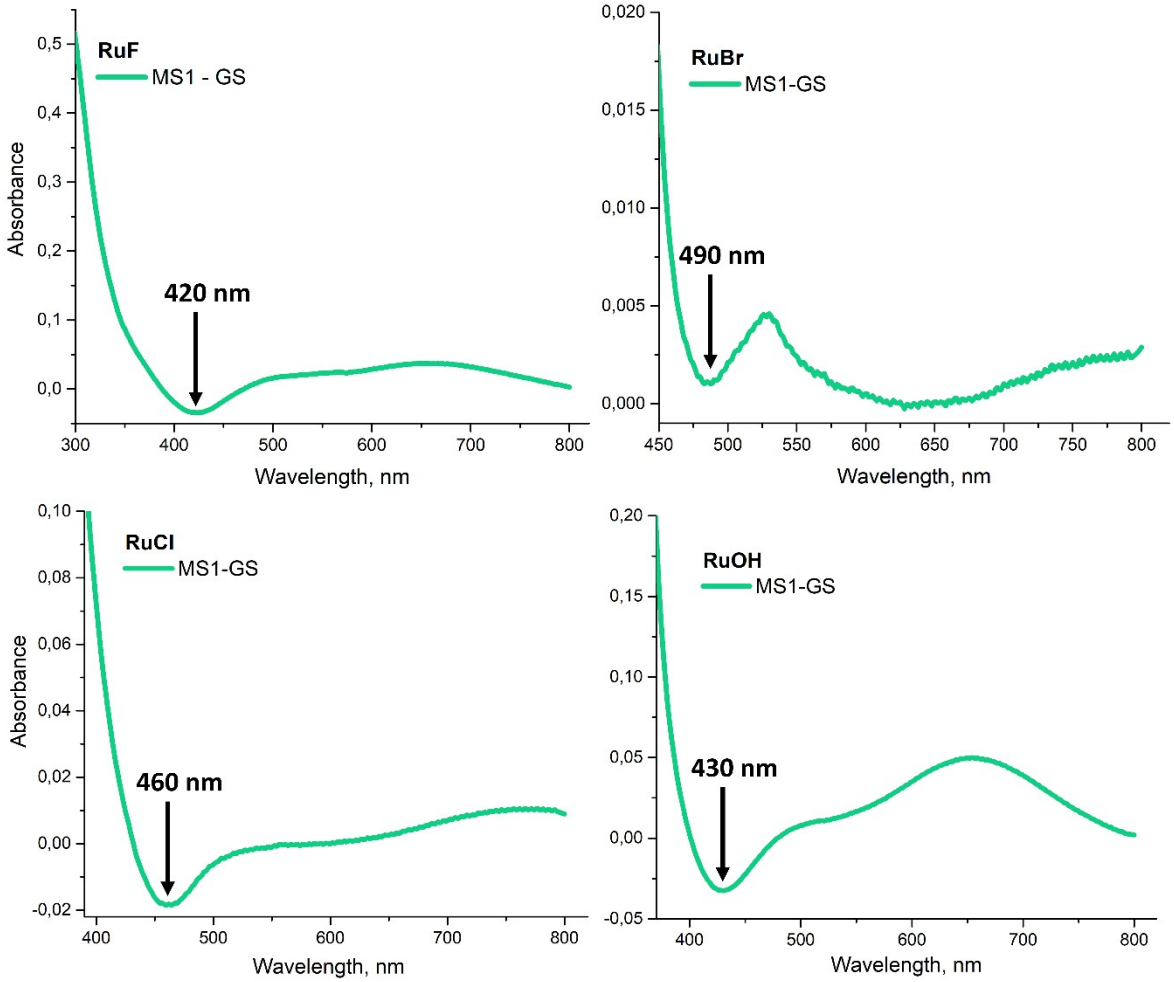

Fig. S4. Difference UV-vis spectra (MS1-GS) of studied compounds at 100 K.

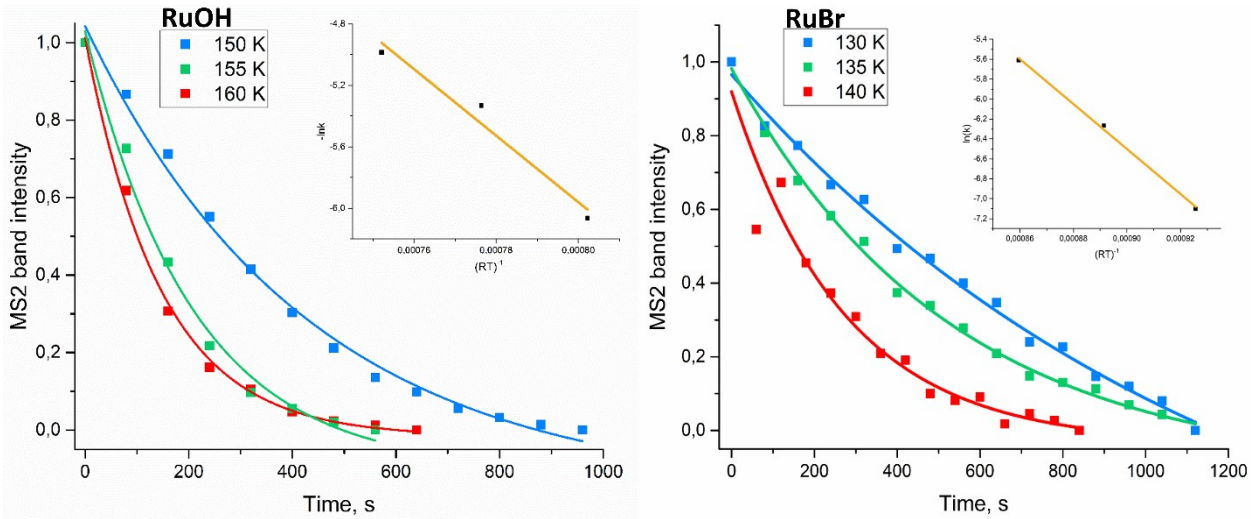

Fig. S5. Isothermal decay of MS2 in **RuOH** and **RuBr** measured by IR-spectroscopy.

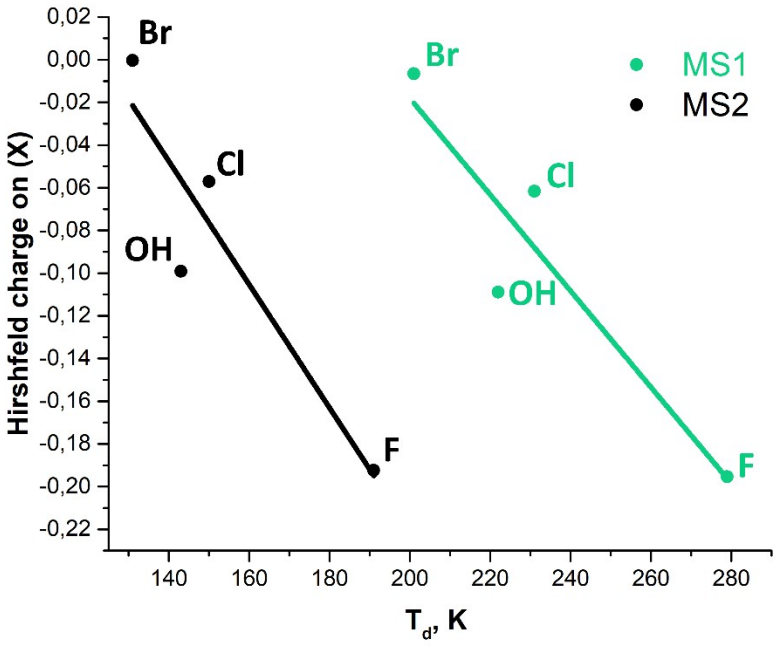

Fig. S6. Correlation of Hirshfeld charge on **X** (NO *trans*-ligand) in MS1 and MS2, and decay temperatures T_d of MS1 and MS2, respectively.

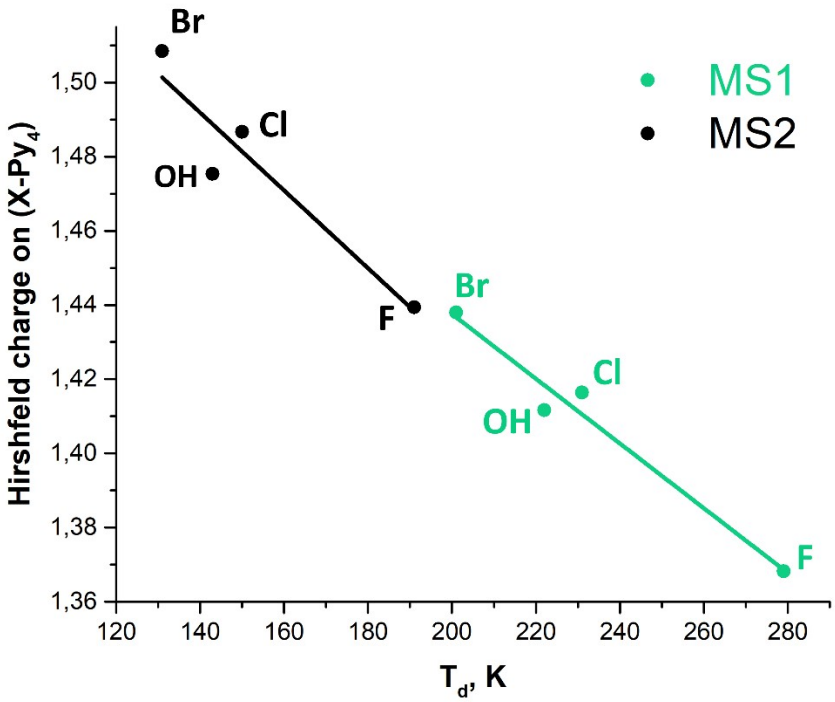

Fig. S7. Correlation of Hirshfeld charge on **X-Py$_4$** in MS1 and MS2, and decay temperatures T_d of MS1 and MS2, respectively.

Table S4. The Hirshfeld charges in GS, MS1 and MS2 on RuNO, X, Py_4 and X-Py_4 groups.

RuNO	GS	MS1	MS2		*X*	GS	MS1	MS2
RuF	0.5913	0.632	0.5604		**RuF**	-0.2084	-0.1954	-0.1924
RuCl	0.5528	0.5837	0.5134		**RuCl**	-0.0931	-0.0616	-0.0571
RuOH	0.5553	0.5883	0.5258		**RuOH**	-0.1276	-0.1089	-0.0991
RuBr	0.5347	0.562	0.4921		**RuBr**	-0.0427	-0.0066	-0.0004
X-Py_4	GS	MS1	MS2		*Py_4*	GS	MS1	MS2
RuF	1.4061	1.3682	1.4394		**RuF**	1.6145	1.5636	1.6318
RuCl	1.4469	1.4164	1.4867		**RuCl**	1.54	1.478	1.5438
RuOH	1.4447	1.4117	1.4754		**RuOH**	1.5723	1.5206	1.5745
RuBr	1.4653	1.438	1.5084		**RuBr**	1.508	1.4446	1.5088

Table S5. The difference of Hirshfeld charges in GS, MS1 and MS2 on RuNO, X, Py_4 and X-Py_4 groups.

RuNO	GS-MS1	GS-MS2		*X*	GS-MS1	GS-MS2
RuF	-0.0407	0.0309		**RuF**	-0.013	-0.016
RuCl	-0.0309	0.0394		**RuCl**	-0.0315	-0.036
RuOH	-0.033	0.0295		**RuOH**	-0.0187	-0.0285
RuBr	-0.0273	0.0426		**RuBr**	-0.0361	-0.0423
X-Py_4	GS-MS1	GS-MS2		*Py_4*	GS-MS1	GS-MS2
RuF	0.0379	-0.0333		**RuF**	0.0509	-0.0173
RuCl	0.0305	-0.0398		**RuCl**	0.062	-0.0038
RuOH	0.033	-0.0307		**RuOH**	0.0517	-0.0022
RuBr	0.0273	-0.0431		**RuBr**	0.0634	-0.0008

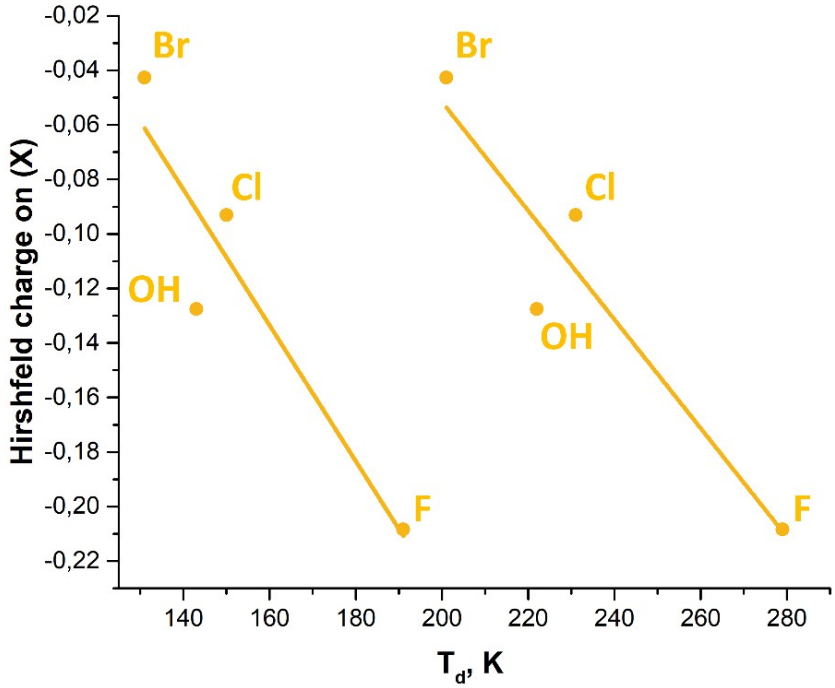

Fig. S8. Correlation of Hirshfeld charge on **X** (NO *trans*-ligand) in GS and decay temperatures T_d of MS1 and MS2.

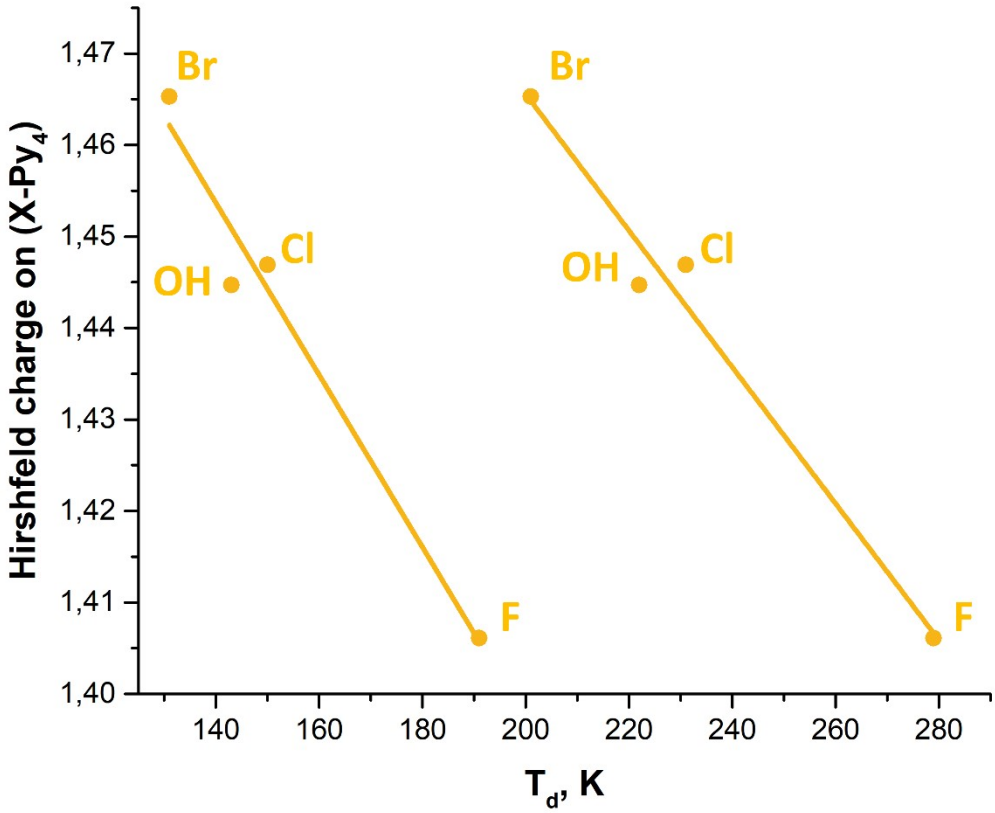

Fig. S9. Correlation of Hirshfeld charge on **X-Py$_4$** in GS and decay temperatures T_d of MS1 and MS2.

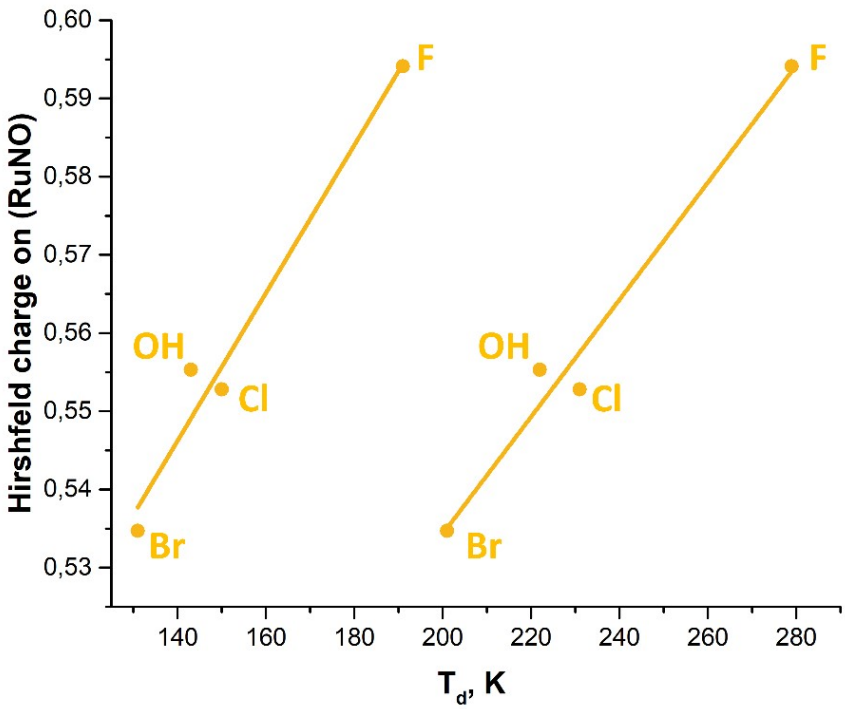

Fig. S10. Correlation of Hirshfeld charge on (RuNO) group in GS and decay temperatures T_d of MS1 and MS2.

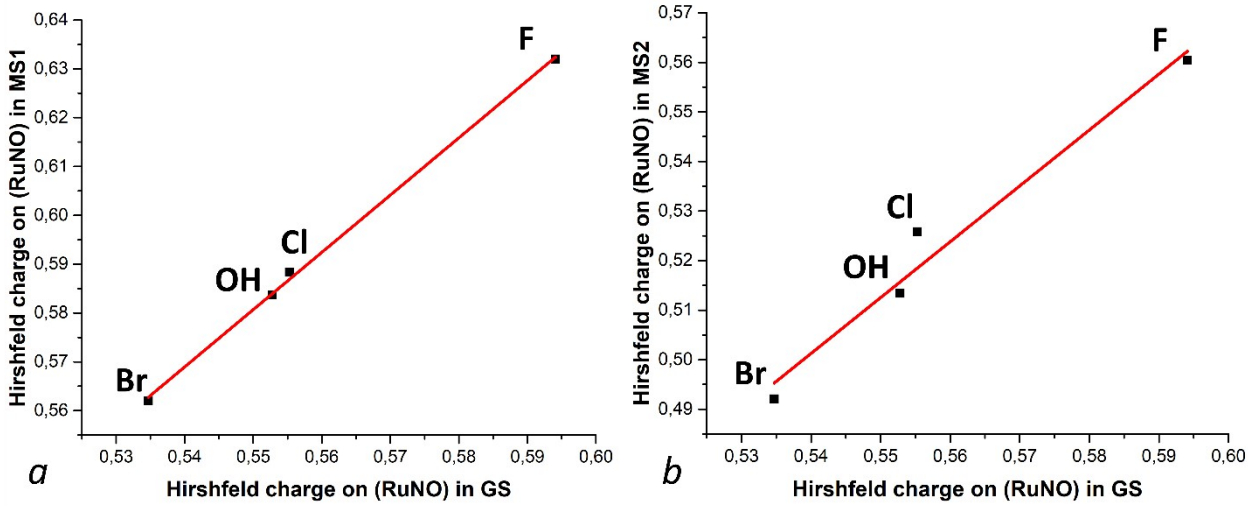

Fig. S11. *a*: correlation of Hirshfeld charges on (RuNO) groups in MS1 and GS; *b*: correlation of Hirshfeld charges on (RuNO) groups in MS2 and GS.

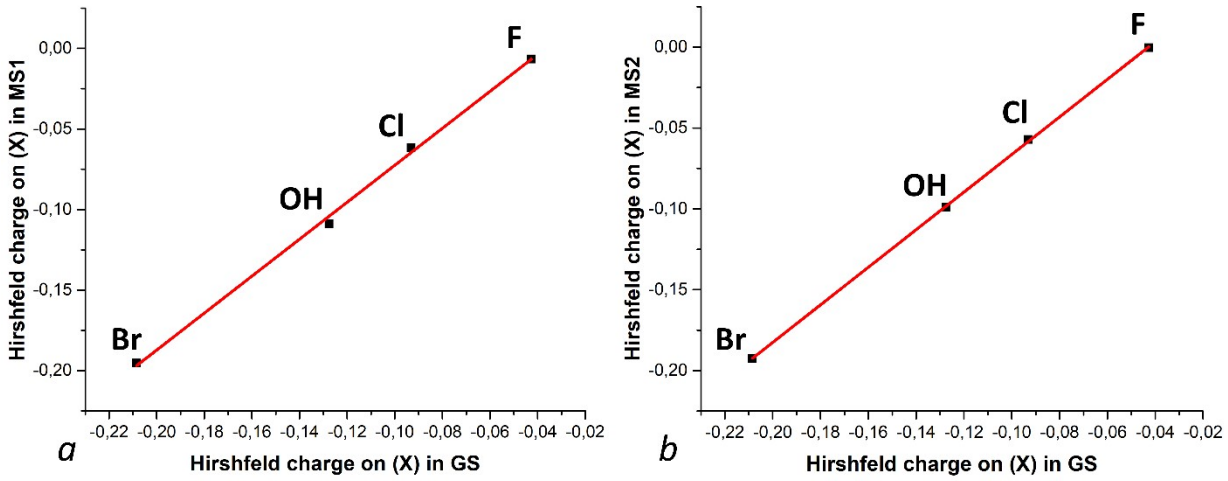

Fig. S12. *a*: correlation of Hirshfeld charges on (**X**) in MS1 and GS; *b*: correlation of Hirshfeld charges on (**X**) in MS2 and GS.

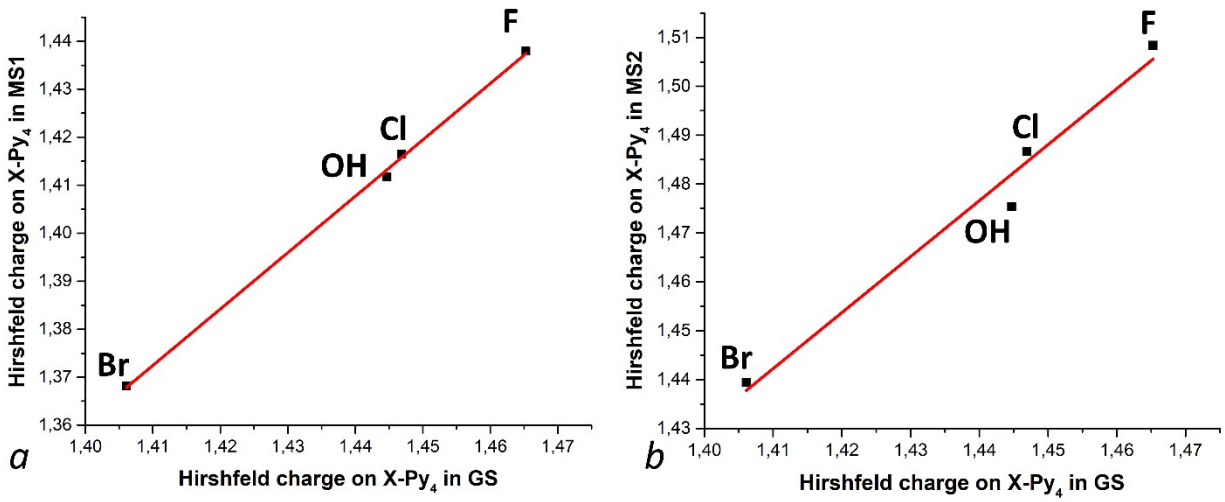

Fig. S13. *a*: correlation of Hirshfeld charges on **X-Py$_4$** in MS1 and GS; *b*: correlation of Hirshfeld charges on **X-Py$_4$** in MS2 and GS.

References

1. Cormary B. et al. Structural Influence on the Photochromic Response of a Series of Ruthenium Mononitrosyl Complexes // Inorg. Chem. 2012. Vol. 51, № 14. P. 7492–7501.

2. Nishimura H. et al. Comparison of the reactivity, electrochemical behaviour, and structure of the trans-bis(acido)tetra(pyridine)nitrosylruthenium cations (acido = hydroxo or chloro) // J. Chem. Soc. Dalt. Trans. 1990. № 1. P. 137.